
DEEP CLUSTERING USING THE SOFT SILHOUETTE SCORE: TOWARDS COMPACT AND WELL-SEPARATED CLUSTERS

Georgios Vardakas

Department of Computer Science and Engineering
University of Ioannina
GR 45110, Ioannina, Greece
g.vardakas@uoi.gr

Ioannis Papakostas

Department of Computer Science and Engineering
University of Ioannina
GR 45110, Ioannina, Greece
john.s.papakostas@gmail.com

Aristidis Likas

Department of Computer Science and Engineering
University of Ioannina
GR 45110, Ioannina, Greece
arly@cs.uoi.gr

ABSTRACT

Unsupervised learning has gained prominence in the big data era, offering a means to extract valuable insights from unlabeled datasets. Deep clustering has emerged as an important unsupervised category, aiming to exploit the non-linear mapping capabilities of neural networks in order to enhance clustering performance. The majority of deep clustering literature focuses on minimizing the inner-cluster variability in some embedded space while keeping the learned representation consistent with the original high-dimensional dataset. In this work, we propose *soft silhouette*, a probabilistic formulation of the silhouette coefficient. Soft silhouette rewards compact and distinctly separated clustering solutions like the conventional silhouette coefficient. When optimized within a deep clustering framework, soft silhouette guides the learned representations towards forming compact and well-separated clusters. In addition, we introduce an autoencoder-based deep learning architecture that is suitable for optimizing the soft silhouette objective function. The proposed deep clustering method has been tested and compared with several well-studied deep clustering methods on various benchmark datasets, yielding very satisfactory clustering results.

Keywords clustering, deep clustering, soft silhouette score, representation learning

1 Introduction

Unsupervised learning has become increasingly important due to the rise of big data collection and the high cost associated with acquiring labeled data. This field of research encompasses various techniques, some of which include generative models [1], representation learning, dimensionality reduction [2] and clustering [3]. Such methods enable us to extract meaningful insight on properties of the data, without relying on explicit guidance or supervision from pre-existing labels. Clustering is a fundamental unsupervised learning task with numerous applications in computer science and many other scientific fields [4–6]. Even though a strict definition of clustering may be challenging to establish, a more flexible interpretation can be stated as follows: Clustering is the process of partitioning a set of objects into groups, known as clusters, such that data in the same group share “common” characteristics while “differing” from data in other groups. While the above clustering definition is simple, it is proven to be a hard machine learning problem [7]. More specifically, it is known that its difficulty arises from several factors like data preprocessing and representation, clustering criterion, optimization algorithm and parameter initialization.

Due to its particular importance, clustering is a well-studied problem with numerous proposed approaches. Generally, they can be classified as hierarchical (divisive or agglomerative), model-based (e.g. k -means [8], mixture models [9]) and density-based (e.g. DBSCAN [10], DensityPeaks [11]). Most methods are effective when the data space is low

dimensional and not complex. Various feature extraction and feature transformation methods have been proposed to map the original complex data to a simpler feature space as a preprocessing step to address those limitations. Some of the methods include Principal Component Analysis [12], Non-negative Matrix Factorization [13], Spectral methods [14], and Minimum Density Hyperplanes [15].

More recently, deep neural networks (DNNs) have been employed for clustering in the context of deep learning. DNNs are used to learn rich and useful data representations from data collections without heavily relying on human-engineered features [16]. They can improve the performance of both supervised and unsupervised learning tasks because of their excellent nonlinear mapping capability and flexibility [17, 18]. Although clustering has not initially been the primary goal of deep learning, several clustering methods have been proposed that exploit the representational power of neural networks; thus, the deep clustering category of methods has emerged. Such methods aim to improve the quality of clustering results by appropriately training neural networks to transform the input data and generate *cluster-friendly* representations, meaning that in the latent space the data will form compact and, in the optimal case, well-separated clusters [19–23].

Several DNN models have been utilized in the deep clustering framework [23]. More specifically, popular architectures include Generative Adversarial Networks [24], Variational Autoencoder [25], Graph Neural Networks [26] and regular DNNs have been utilized by methods such as ClusterGan [27], VaDE [28], JULE [29], NIMLC [30].

However, the majority of the methods rely on training Autoencoders (AE), which is the most utilized deep learning model for clustering. AE-based deep clustering methodologies attempt to exploit the non-linear capabilities of the encoder and decoder models in order to assist in latent space [31]. To achieve this goal, novel objective functions have been proposed that integrate the typical AE reconstruction error with a clustering loss in order to train the AE network so that in the learned embedded space, the data will form more compact clusters (achieved through minimization of a clustering objective), while at the same time retaining the information of the original data (achieved by minimizing the AE reconstruction error).

As presented in the related work section, the vast majority of AE-based methods learn a representation in which individual clusters have small inner cluster variability. Most common approaches are the minimization of the k -means error, or the KL divergence between the soft clustering assignments and a target distribution. Such a representation has been shown to improve the clustering results in several scenarios. However, minimizing only the inner cluster distance is a suboptimal strategy. Our motivation is to formulate a deep clustering objective that simultaneously considers both the inner cluster distance and the outer cluster separation. This is achieved by optimizing the *soft silhouette* objective introduced in this work.

Assessing the quality of a clustering solution is typically a challenging task. In this direction, several quality measures have been proposed which can be categorized as external and internal measures [32]. External quality measures, as the name suggests, use additional information about the data as the ground truth labels. Well-known external evaluation measures include Normalized Mutual Information (NMI) [33], Adjusted Mutual Information (AMI) [34], Adjusted Rand Index and (ARI) [35, 36]. However, such measures are not applicable in real-world applications where the ground truth labels are absent. Internal quality measures, on the other hand, can be applied to the clustering problem since they are based solely on the information intrinsic to the data. Some typical internal clustering measures that take into account both cluster compactness and separation are the Dunn index [37], the Calinski-Harabasz index [38], the Davies-Bouldin index [39], and the silhouette [40]. In particular, the silhouette coefficient is the most widely used and successful internal validation measure [41].

The typical silhouette is considered as an effective clustering quality measure that combines both inter and intra cluster information. Specifically, silhouette rewards clustering solutions that exhibit both compactness within individual clusters and clear separation between clusters. However, it assumes a hard clustering solution, thus it cannot be used to evaluate probabilistic clustering solutions, unless they are transformed to discrete ones based on maximum cluster membership probability. In addition, the silhouette score cannot be efficiently used as a clustering objective for neural network training since it is not differentiable.

In this work, in order to overcome the above limitations, we propose an extension of the silhouette score, called *soft silhouette* score, that evaluates the quality of probabilistic clustering solutions without requiring their transformation to discrete ones. Besides this obvious advantage, a notable property of soft silhouette is that it is differentiable with respect to cluster assignment probabilities. Assuming that such probabilities are provided by a parametric machine learning model, the soft silhouette score can be used as a clustering objective function to train parametric probabilistic models using typical gradient-based approaches.

To this end, we propose a novel AE-based deep clustering methodology that directly provides cluster assignment probabilities as network outputs and exploits the soft silhouette score as a clustering objective. In this way, by train-

ing the network using soft silhouette, we achieve minimization of the inter-cluster variance, while at the same time maximizing the margin between clusters in the embedded space.

The rest of the paper is organized as follows. In Section 2, we give a brief overview of the deep clustering methods based on the AE model, while in Section 3 the soft silhouette score introduced. Then in Section 4 we describe the proposed deep clustering methodology by presenting the model architecture, the corresponding objective function as well as the training method. Finally, in Section 5, we provide extensive experimental results and comparisons, while in Section 6, we provide conclusions and future work suggestions.

2 Deep Clustering using Autoencoders

The autoencoder (AE) constitutes the most widely used model in deep clustering methodologies [23]. It consists of an encoder network $z = f_\theta(x)$ which given an input x provides embedding z , and the decoder network $\hat{x} = g_w(z)$ that provides the reconstruction \hat{x} given the embedding z . In the typical autoencoder case, given a dataset $X = \{x_1, \dots, x_N\}$, the parameters θ and w are adjusted by minimizing the reconstruction loss:

$$\mathcal{L}_{rec} = \frac{1}{N} \sum_{i=1}^N \|x_i - g_\theta(f_w(x_i))\|^2 \quad (1)$$

A straightforward approach for AE-based clustering is to first train the AE using the reconstruction loss and then cluster the embeddings $z_i = f_w(x_i)$ using any clustering method. Thus data projection and clustering are performed independently. However, it has been found the better results are obtained if the embeddings are formed taking into account both reconstruction and clustering.

Therefore, the *AE clustering framework* has emerged, where the goal is to create cluster-friendly embeddings z_i . To achieve this goal, the reconstruction loss is enhanced with an appropriately defined clustering loss \mathcal{L}_{cl} resulting in a total loss of the form:

$$\mathcal{L}_{AE} = \mathcal{L}_{rec} + \lambda \mathcal{L}_{cl}, \quad (2)$$

where the hyperparameter λ balances the relative importance the two objectives.

It should be noted that the of minimization clustering loss enforces the formation of embeddings z_i with small cluster variance. An easily obtained trivial solution exists, where all data points x_i are mapped to embeddings z_i that are all very close to each other (ie. the encoder is actual a constant function). To avoid this trivial solution the reconstruction loss is added that forces the embeddings z_i to retain the information of the original dataset. In essence, AE clustering methods strive to create embeddings that form compact clusters, while keeping the characteristics of the original dataset. The most widely used AE-based methods are summarized next.

Inspired by the *t*-SNE [42] algorithm, the Deep Embedding Clustering (DEC) [43] method has been proposed that optimizes both the reconstruction objective and a clustering objective. DEC transforms the data in the embedded space using an autoencoder and then optimizes a clustering loss defined by the *KL* divergence between two distributions p_{ij} and q_{ij} : q_{ij} are soft clustering assignments of the data based on the distances in the embedded space between data points and cluster centers, and p_{ij} is an adjusted target distribution aiming to enhance the clustering quality by leveraging the soft cluster assignments. More specifically, q_{ij} is defined as

$$q_{ij} = \frac{(1 + \|z_i - \mu_j\|^2/\alpha)^{-\frac{\alpha+1}{2}}}{\sum_{j'} (1 + \|z_i - \mu_{j'}\|^2/\alpha)^{-\frac{\alpha+1}{2}}}, \quad (3)$$

where $z_i = f_w(x_i)$, μ_j is a cluster center in the embedded space and α is the degrees of freedom. Additionally, $p_{ij} = \frac{q_{ij}^2/f_{ij}}{\sum_{j'} q_{ij}^2/f_{ij}}$ (with $f_{ij} = \sum_i q_{ij}$) is the target probability distribution that aims to sharpen the cluster probability assignments.

A modification of this method is the Improved Deep Clustering with local structure preservation (IDEC) [44]. Both DEC and IDEC optimize the same objective function:

$$\mathcal{L}_{rec} + \lambda \sum_{i=1}^n \sum_{j=1}^k p_{ij} \log \frac{p_{ij}}{q_{ij}}. \quad (4)$$

Specifically, DEC performs pretraining to minimize the reconstruction loss and subsequently excludes the decoder part of the network, focusing solely on the clustering loss during the training phase. In contrast, IDEC simultaneously

optimizes both the reconstruction loss and the clustering loss during the training phase of the AE. From eq. 3 and eq. 4 it is clear that the above approaches aim to minimize only an inner cluster distance loss.

Similar to DEC, the Deep Clustering Network (DCN) [31] jointly learns the embeddings and the cluster assignments by directly optimizing the k -means clustering loss on the embedded space. The optimized objective function is:

$$\mathcal{L}_{rec} + \lambda \sum_{i=1}^n \|z_i - Ms_i\|^2 \quad (5)$$

where $z_i = f_w(x_i)$, M is a matrix containing the k cluster centers in the embedded space, and s_i is the cluster assignment vector for data point x_i with only one non-zero element. An analogous early work is Autoencoder-based data clustering (AEC) [45] which also aims to minimize the distance between embedded data and their nearest cluster centers.

3 The soft silhouette score

3.1 Silhouette

The silhouette score [40] is a measure utilized to assess the quality of a clustering solution. It assumes that a good clustering solution encompasses compact and well-separated clusters. Assume we are given a partition $C = \{C_1, \dots, C_K\}$ of a dataset $X = \{x_1, \dots, x_N\}$ into K clusters. Let also $d(x_i, x_j)$ denote the distance between x_i and x_j .

The silhouette score computation proceeds by evaluating the individual silhouette score $s(x_i)$ of each data point x_i as follows. We first compute its average distance $a(x_i)$ to all other data points within its cluster C_I :

$$a(x_i) = \frac{1}{|C_I| - 1} \sum_{x_j \in C_I, i \neq j} d(x_i, x_j), \quad (6)$$

where $|C_I|$ represents the cardinality of cluster C_I , where $|C_I| > 1$. The value of $a(x_i)$ value quantifies how well the datapoint x_i fits within its cluster. A low value of $a(x_i)$ indicates that x_i is similar to its cluster members, suggesting that x_i is probably grouped correctly. Conversely, a higher value of $a(x_i)$ indicates that x_i is far from its cluster members.

The silhouette score also requires the calculation of the minimum average outer-cluster distance $b(x_i)$ for each datapoint $x_i \in C_I$ defined as

$$b(x_i) = \min_{J \neq I} \frac{1}{|C_J|} \sum_{x_j \in C_J} d(x_i, x_j). \quad (7)$$

A large $b(x_i)$ value indicates that the datapoint x_i significantly differs from datapoints in other clusters which is desirable.

The silhouette score of a datapoint x_i takes into account the requirements for small $a(x_i)$ and large $b(x_i)$ and is defined as:

$$s(x_i) = \frac{b(x_i) - a(x_i)}{\max\{a(x_i), b(x_i)\}}. \quad (8)$$

It should be noted that $-1 \leq s(x_i) \leq 1$. A value close to 1 is achieved when $a(x_i)$ is small and $b(x_i)$ is high. This indicates that x_i has been assigned to a compact, well-separated cluster. In contrast, a value close to -1 suggests that the x_i is more similar to points in other clusters than to points in its cluster, thus it has been probably assigned a wrong cluster label.

The total silhouette score for the whole partition C of the dataset X is obtained by aggregating the individual silhouette values through typical averaging:

$$S(X) = \frac{1}{N} \sum_{i=1}^N s(x_i) \quad (9)$$

The silhouette score [40] is not only suitable for (internal) clustering evaluation but also defines an intuitive clustering objective that rewards compact and well-separated clusters. As presented in related work, while several deep clustering objectives aim to provide compact clustering solutions, they do not optimize explicitly for cluster separability. Next, we introduce a probabilistic silhouette score, termed soft silhouette, which allows us to optimize for both compact and well-separated clusters.

3.2 Soft Silhouette

The soft silhouette score introduced below constitutes an extension of the typical silhouette score that assumes probabilistic cluster assignments instead of hard cluster assignments. More specifically, assume a dataset $X = \{x_1, \dots, x_N\}$ partitioned into K clusters $C = \{C_1, \dots, C_K\}$ and let $d(x_i, x_j)$ the distance between data points x_i and x_j . Let also $P_{C_I}(x_i)$ denote the probability that x_i belongs to cluster C_I . Obviously $\sum_{I=1}^K P_{C_I}(x_i) = 1$.

Assuming that x_i belongs to cluster C_I we define as:

- $a_{C_I}(x_i)$ the value of the distance of x_i to cluster C_I . This is actually a weighted average (expected value) of the distances of x_i to all other points $x_j \in X$ with weight the probability $P_{C_I}(x_j)$ (ie. that x_j belongs to the cluster of interest C_I).

$$a_{C_I}(x_i) = \frac{\sum_{j=1}^N P_{C_I}(x_j) d(x_i, x_j)}{\sum_{j=1, j \neq i}^N P_{C_I}(x_j)} \quad (10)$$

- $b_{C_I}(x_i)$ the minimum value of the (expected) distance of x_i from the other clusters C_j different from C_I .

$$b_{C_I}(x_i) = \min_{J \neq I} \frac{\sum_{j=1}^N P_{C_J}(x_j) d(x_i, x_j)}{\sum_{j=1, j \neq i}^N P_{C_J}(x_j)} = \min_{J \neq I} a_{C_J}(x_i) \quad (11)$$

- $s_{C_I}(x_i)$ the conditional silhouette value for x_i given that it belongs to cluster C_I :

$$s_{C_I}(x_i) = \frac{b_{C_I}(x_i) - a_{C_I}(x_i)}{\max\{a_{C_I}(x_i), b_{C_I}(x_i)\}} \quad (12)$$

Then the soft silhouette value $sf(x_i)$ of data point x_i is computed as the expected value of $s_{C_I}(x_i)$ with respect to its cluster assignment probabilities $P_{C_I}(x_i)$:

$$sf(x_i) = \sum_{i=1}^K P_{C_I}(x_i) s_{C_I}(x_i) \quad (13)$$

and the total soft silhouette score $Sf(X)$ of the partition is computed by aggregating (averaging) the individual scores $sf(x_i)$:

$$Sf(X) = \frac{1}{N} \sum_{i=1}^N sf(x_i), \quad (14)$$

It should be noted that in the case of hard clustering, the cluster assignment probability vectors become one-hot vectors and the soft silhouette equations become similar to the typical silhouette equations.

It is obvious from the above equations that soft silhouette is differentiable with respect to the cluster assignment probabilities. Therefore it can be employed as a clustering objective function to be optimized in a deep learning framework. The major advantage of this objective is that it optimizes simultaneously both cluster compactness and separation. Such a deep clustering approach is presented next.

4 The DCSS method: Deep Clustering using Soft Silhouette

In this section we propose the Deep Clustering using Soft Silhouette (DCSS) algorithm which belongs the category of AE-based deep clustering methods that employs soft silhouette as a clustering loss.

As described in Section 2 a typical AE-based deep clustering method employs an encoder network

$$z = f_w(x), \quad f_w(\cdot) : \mathbb{R}^d \rightarrow \mathbb{R}^m,$$

that provides the latent representations (embeddings) z and a decoder network

$$\hat{x} = g_\theta(x), \quad g_\theta(\cdot) : \mathbb{R}^m \rightarrow \mathbb{R}^d,$$

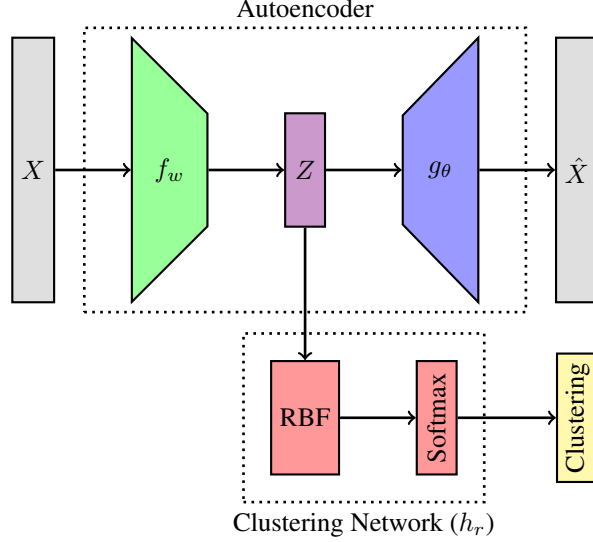


Figure 1: The proposed model architecture.

that reconstructs the outputs given the embeddings. The networks are trained to optimize a total loss that is the sum of the reconstruction loss and the clustering loss: $\mathcal{L}_{AE} = \mathcal{L}_{rec} + \lambda \mathcal{L}_{cl}$.

In the proposed approach the clustering loss will be based on the soft silhouette score, which requires the cluster assignment probabilities $p(x) = (p_1(x), \dots, p_K(x))$ for an input x . For this reason, we enrich the AE-model with an additional network $h_r(z)$, called clustering network, that takes as input the embedding $z = f_w(x)$ of a data point x and outputs the cluster assignment probabilities $p_j(x) = h_{rj}(x)$ for $j = 1, \dots, K$. Therefore, given the dataset $X = \{x_1, \dots, x_N\}$, the embedding $z_i = f_w(x_i)$ are first computed. Then the pairwise distances $d(z_i, z_j)$ and the cluster assignment probability vectors $p(x_i) = h_r(z_i)$ are specified, required for the soft silhouette computation.

The proposed three network architecture is illustrated in Fig. 1. It can be observed that the clustering network operates in parallel with the decoder network. For an input vector x the model provides the embedding vector z , the reconstruction vector \hat{x} and the probability vector $p(x)$.

Based on the experimentation with several alternatives, we have selected as clustering network h_r an a Radial Basis Function (RBF) [46] model with a softmax output unit that provides the probability vector of the cluster assignments. The number of RBF units is set equal to the number of clusters K .

Soft silhouette is a criterion that should maximized in order to obtain solutions of good quality. Since a clustering loss is a quantity to be minimized, we take into account that $Sf \leq 1$ and define the clustering loss as follows:

$$\mathcal{L}_{cl} = 1 - Sf \quad (15)$$

Note that L_{cl} is always positive and attains each minimum value when Sf is maximum ($Sf = 1$). Thus the total loss for model training is specialized as follows:

$$L_{AE} = \frac{1}{N} \sum_{i=1}^N \|x_i - g_\theta(f_w(x_i))\|^2 + \lambda(1 - Sf(h_r(X))) \quad (16)$$

where $h_r(X) = \{h_r(x_1), \dots, h_r(x_N)\}$ are the cluster assignment probability vectors. It should be noted that the pairwise distances $d(f_w(x_i), f_w(x_j))$ between the embeddings are also involved in the Sf computation. In this work the Euclidean distance has been used. Since L_{AE} is differentiable with respect to the model parameters w, θ, r it can be minimized using typical gradient-based procedures.

A technical issue that has emerged when training the model is that in many cases a trivial solution is attained where the output probabilities tend to be uniform (ie. equal to $1/K$) for many data points. To overcome this difficulty, we have included an additional term to the objective function that penalizes uniform solutions by minimizing the entropy of the output probability vectors. Thus, the entropy regularization term L_{reg} is defined as follows:

$$H(h_r(X)) = - \sum_{i=1}^N \sum_{j=1}^K h_{rj}(x_i) \log h_{rj}(x_i) \quad (17)$$

Algorithm 1 Deep Clustering using Soft Silhouette algorithm (DCSS)

Require: X (dataset)**Require:** K (number of clusters)**Require:** λ_1, λ_2 (regularization hyperparameters)

1: Randomly initialize the w and θ AE parameters.**Stage 1: Pretraining**2: Pretrain the encoder f_w and decoder g_θ by minimizing the reconstruction error \mathcal{L}_{rec} (eq. 1) through gradient based optimization for T_{pr} epochs. \triangleright We employed batch training using the Adam optimizer.3: Apply k -means with K clusters to the learned representations $z = f_w(X)$.4: Initialize the parameters of the clustering network h_r using the k -means result.**Stage 2: Training**5: Update the parameters θ, w and r by minimizing the total loss (eq. 18) until convergence through gradient based optimization to obtain θ^*, w^* and r^* . \triangleright We employed batch training using the Adam optimizer.**Stage 3: Inference**6: Compute the clustering solution $C = \arg \max softmax(h_{r^*}(f_{w^*}(X)))$. \triangleright Data clustering.7: **return** the clustering solution C and the learned parameters w^*, θ^*, r^* .

The final total loss that is minimized to train our model is:

$$\mathcal{L}_{AE} = \mathcal{L}_{rec} + \lambda_1 \mathcal{L}_{cl} + \lambda_2 \mathcal{L}_{reg} \quad (18)$$

and in more detail

$$\mathcal{L}_{AE} = \frac{1}{N} \sum_{i=1}^N \|x_i - g_\theta(f_w(x_i))\|^2 + \lambda_1 (1 - Sf(h_r(X))) - \lambda_2 \frac{1}{N} \sum_{i=1}^N \sum_{j=1}^K h_{rj}(x_i) \log h_{rj}(x_i) \quad (19)$$

The details of approach, called Deep Clustering using Soft Silhouette (DCSS), are summarized in Algorithm 1.

5 Experiments

In this section we present our experimental results on both real datasets and a synthetic dataset. In the first part, we demonstrate the representation learning capabilities of several methods compared to DCSS on a synthetic dataset. In the second part, we demonstrate the deep clustering capabilities of the DCSS method on several real datasets compared to the most widely used (AE-based) deep clustering methods that have been discussed in Section 2.

5.1 Synthetic Data Demonstration

We have relied on the synthetic dataset considered in [31] (for testing the DCN method) generated as follows. Let's suppose the observed high dimensional data points x_i exhibit a clear cluster structure in a two-dimensional latent space Z , ie. the latent vectors $z_i \in \mathbb{R}^2$ form compact and well-separated clusters. Given a latent vector z_i , the corresponding observation x_i is generated using the following transformation:

$$x_i = \sigma(U\sigma(Wz_i)), \quad (20)$$

where $W \in \mathbb{R}^{10 \times 2}$ and $U \in \mathbb{R}^{100 \times 10}$ are matrices whose entries are sampled from the Normal distribution $\mathcal{N}(0, 1)$, and $\sigma(x)$ is the logistic function that introduces non-linearity into the generation process. Given the observations x_i , recovering the original clustering-friendly domain in which z_i resides appears challenging.

We generated a set of latent vectors z_i belonging to four planar clusters, each with 2,500 samples (as shown in the first subfigure of Fig. 2) and we computed the corresponding observations x_i . The rest subfigures Fig. 2 demonstrate the two-dimensional projections provided using several dimensionality reduction methods given the observations x_i as input. More specifically, we present the solutions provided by Principal Component Analysis (PCA) [12], Singular Value Decomposition (SVD), Non-negative Matrix Factorization (NMF) [13], Local Linear Embeddings (LLE) [47], Isomap [48], t-SNE [42] and Laplacian Eigenmap (LapEig), which is the first algorithmic step of the spectral clustering method [14]. We also considered the deep clustering methods DEC [43], IDEC [44], DCN [31], as well as our proposed DCSS method.

It is evident that the projection methods that do not optimize a clustering loss (first and second rows) have failed to reveal the hidden two-dimensional latent structure. On the contrary, deep clustering methods (bottom row) demonstrated better performance. Specifically, DEC was able to recover three out of four latent clusters, however the fourth

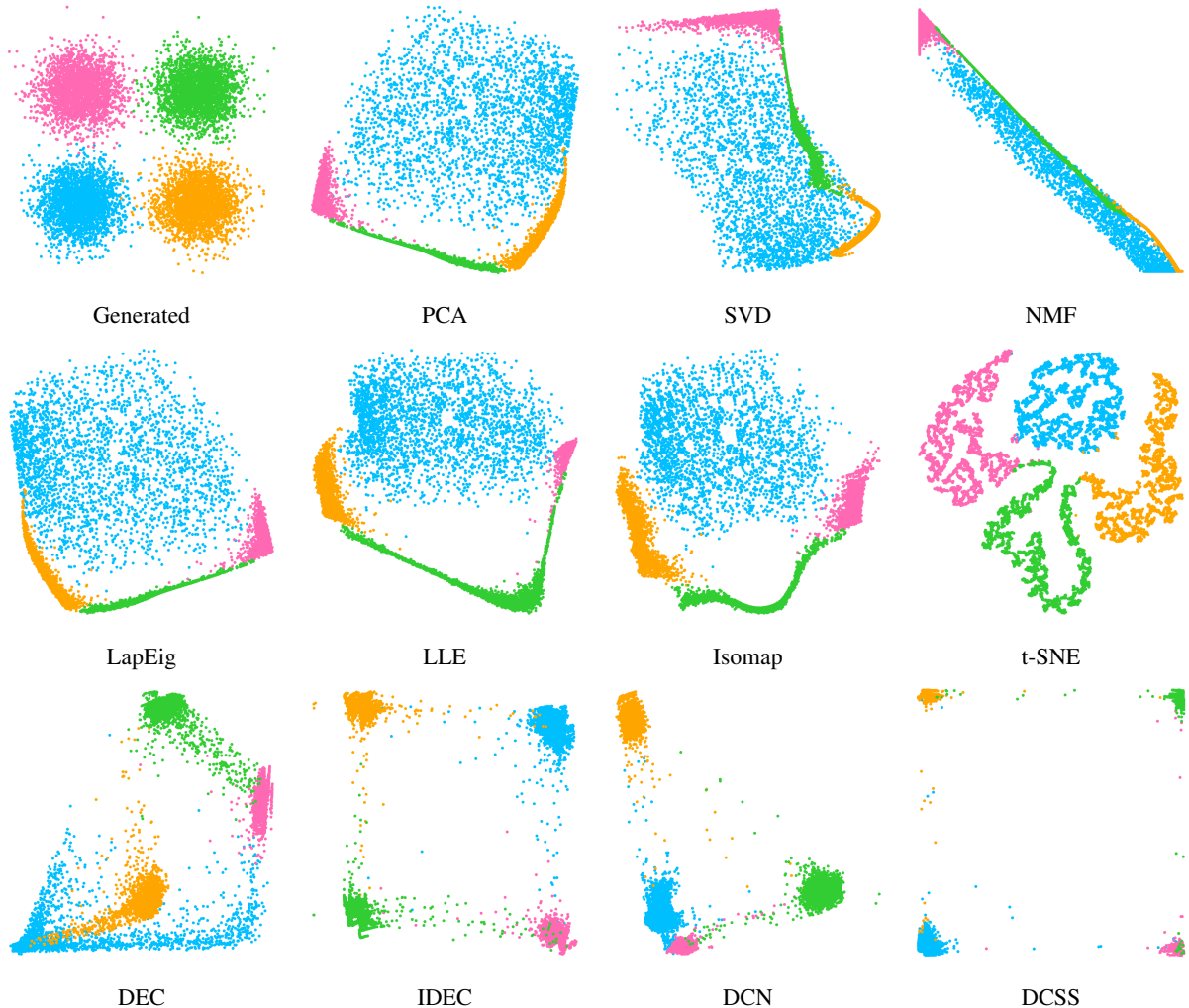


Figure 2: Synthetic demonstration of the representation learning capabilities of several methods. The generated 2-d dataset (top left) is hidden from the methods. Each method receives as input a 100-d dataset generated by non-linear transformations applied to the original 2-d data and provides a 2-d latent representation of the 100-d dataset, which is presented in the plots. Color indicates the true cluster labels.

was scattered. DCN was able to reconstruct all of them, but the blue and red clusters are not sufficiently separated. IDEC was able to learn a very informative projection revealing the four cluster structure. Superior are the results of the DCSS method, which was not only able to reveal the four clusters, but also sufficiently maximized their separation.

5.2 Datasets

Table 1 summarizes the benchmark datasets that we used for experimental evaluation, which vary in size n , dimensions d , number of clusters k , complexity, data type, and domain of origin. The subsequent paragraphs offer a more comprehensive overview of the datasets we employed and outline the preprocessing procedures we implemented for each of these datasets.

The datasets used in this study include the Pendigits (PEN), EMNIST MNIST (E-MNIST), and EMNIST Balanced Digits (BD). These datasets consist of handwritten digits categorized into ten classes, each representing digits from 0 to 9. It is worth noting that the EMNIST dataset constitutes an extended and more challenging version of the MNIST dataset [49]. Both the E-MNIST and BD datasets comprise images with a resolution of 28×28 pixels. In contrast, Pendigits data instances are represented by 16-dimensional vectors containing pixel coordinates.

Table 1: The datasets used in our experiments. N is the number of data instances, d is the dimensionality, and k denotes the number of clusters.

Dataset	Type	N	d	k	Source
EMNIST Balanced Digits	Image	28000	28×28	10	[51]
EMNIST MNIST	Image	70000	28×28	10	[51]
EMNIST Balanced Letters (A-J)	Image	28000	28×28	10	[51]
EMNIST Balanced Letters (K-T)	Image	28000	28×28	10	[51]
EMNIST Balanced Letters (U-Z)	Image	16800	28×28	6	[51]
HAR	Tabular	10299	560	6	[52]
Pendigits	Tabular	10992	16	10	[53]
Waveform-v1	Tabular	5000	21	3	[53]
Synthetic	Tabular	10000	2	4	[31]

In addition, the EMNIST Balanced Letters (BL) dataset is included, featuring handwritten letters in both uppercase and lowercase forms, with a resolution of 28×28 pixels. The BL dataset has been divided into three mutually exclusive subsets. The first subset contains the letters A to J, the second includes the letters K to T, and the last subset contains the remaining letters U to Z. The first two subsets comprise 28000 data points each, distributed across 10 clusters, while the last subset consists of 16800 data points and 6 clusters. The Human Activity Recognition with Smartphones (HAR) dataset was also considered. This dataset consists of data collected from the accelerometer and gyroscope sensors of smartphones, sampled during a human activity. Specifically, each record in the dataset is a 560 feature vector with time and frequency domain variables. In addition, HAR consists of 6 classes of human activities which are the following: walking, walking upstairs, walking downstairs, sitting, standing, laying. Furthermore, the Waveform-v1 (WVF-v1) dataset was included which consists of 3 classes of generated waves with 5000 datapoints. Each class is generated from a combination of 2 of 3 ‘base’ waves. Finally, we also report results for the synthetic dataset described in the previous subsection.

In all datasets, we used min-max normalization as a preprocessing step, to map the attributes of each data point to the $[0, 1]$ interval to prevent attributes with large ranges from dominating the distance calculations and avoid numerical instabilities in the computations [50].

5.3 Neural Network Architectures

Determining optimal architectures and hyperparameters through cross-validation is not feasible in unsupervised learning problems. Therefore, we opt for commonly used architectures for the employed neural network models while avoiding dataset-specific tuning. Regarding tabular data, our approach involves adopting a well-established architecture, which consists of fully connected layers [43, 54]. The specific AE architecture that we used is the following:

$$x_d \rightarrow \text{Fc}_{500} \rightarrow \text{Fc}_{500} \rightarrow \text{Fc}_{2000} \rightarrow \text{Fc}_m \rightarrow \text{Fc}_{2000} \rightarrow \text{Fc}_{500} \rightarrow \text{Fc}_{500} \rightarrow \hat{x}_d,$$

where Fc_m stands for fully connected layer with m neurons and x_d represents a d -dimensional data vector.

In what concerns image datasets, convolutional Neural Networks (CNNs) have demonstrated superior effectiveness in capturing semantic visual features. Consequently, we exploit a convolutional-deconvolutional AE to learn the embeddings for the image datasets. The AE architecture consists of three convolutional layers (encoder), one fully connected layer (embedding layer), and three deconvolutional layers (decoder) [55–57]. More specifically, the architecture is the following:

$$x_{28 \times 28} \rightarrow \text{Conv}_{32}^5 \rightarrow \text{Conv}_{64}^5 \rightarrow \text{Conv}_{128}^3 \rightarrow \text{Fc}_m \rightarrow \text{Deconv}_{128}^3 \rightarrow \text{Deconv}_{64}^5 \rightarrow \text{Deconv}_{32}^5 \rightarrow \hat{x}_{28 \times 28},$$

where Conv_b^a (Deconv_b^a) denote a convolutional (deconvolutional) layer with an $a \times a$ kernel and b filters, while the stride always set to 2.

In the above encoder-decoder networks, the ReLU activation function is used [58], except for the embedded layer of the AE, where the Hyperbolic Tangent (tanh) function is used. Weights and biases are initialized using the He initialisation method [59].

As already mentioned, in what concerns the clustering network, a Radial Basis Function (RBF) model has been selected with the number of hidden units equal to the number of clusters. The outputs of the RBF units are fed to a K -output softmax activation function that provides the cluster assignment probabilities. After the AE pre-training, we initialize the centers of the RBF layer by using the k -means algorithm in the embedded space, while we initialize σ to a small positive value. The temperature parameter T of the softmax was set equal to $T = 20$.

Table 2: Performance results of the compared clustering methods.

Dataset	Measure	Method					
		k -means	AE + k -means	DCN	DEC	IDEC	DCSS
BD	NMI	0.48	0.72±0.01	0.75±0.02	0.80±0.03	0.82±0.01	0.86±0.04
	ARI	0.36	0.65±0.02	0.63±0.05	0.75±0.06	0.77±0.01	0.80±0.07
BL (A-J)	NMI	0.35	0.65±0.02	0.68±0.03	0.77±0.03	0.77±0.03	0.80±0.02
	ARI	0.25	0.55±0.02	0.56±0.05	0.69±0.06	0.69±0.05	0.72±0.04
BL (K-T)	NMI	0.51	0.73±0.02	0.77±0.03	0.84±0.01	0.84±0.02	0.90±0.02
	ARI	0.43	0.67±0.04	0.69±0.06	0.81±0.02	0.81±0.04	0.87±0.03
BL (U-Z)	NMI	0.47	0.64±0.01	0.64±0.02	0.68±0.02	0.67±0.02	0.71±0.04
	ARI	0.41	0.60±0.02	0.56±0.04	0.65±0.03	0.63±0.02	0.68±0.06
E-MNIST	NMI	0.48	0.75±0.01	0.83±0.03	0.84±0.03	0.85±0.02	0.88±0.04
	ARI	0.36	0.69±0.01	0.78±0.04	0.80±0.04	0.81±0.03	0.83±0.06
HAR	NMI	0.59	0.67±0.06	0.77±0.01	0.74±0.06	0.74±0.10	0.81±0.06
	ARI	0.46	0.60±0.09	0.70±0.02	0.66±0.08	0.65±0.12	0.74±0.09
PEN	NMI	0.69	0.68±0.02	0.73±0.03	0.73±0.03	0.75±0.03	0.78±0.02
	ARI	0.56	0.59±0.04	0.62±0.05	0.62±0.05	0.65±0.04	0.68±0.04
WVF-v1	NMI	0.74	0.84±0.13	0.95±0.08	0.93±0.12	0.89±0.09	1.00±0.00
	ARI	0.70	0.87±0.13	0.95±0.09	0.93±0.14	0.91±0.08	1.00±0.00
Synthetic	NMI	0.82	0.72±0.14	0.79±0.09	0.91±0.08	0.90±0.10	0.93±0.10
	ARI	0.83	0.70±0.19	0.75±0.14	0.92±0.12	0.91±0.11	0.93±0.10

5.4 Evaluation

It is important to mention that since clustering is an unsupervised problem, we ensured that all algorithms were unaware of the true clustering of the data. In order to evaluate the results of the clustering methods, we use standard external evaluation measures, which assume that ground truth clustering is available [32]. For all algorithms, the number of clusters is set to the number of ground-truth categories and assumes ground truth that cluster labels coincide with class labels. The first evaluation measure is the *Normalized Mutual Information* (NMI) [33] defined as:

$$NMI(Y, C) = \frac{2 \times I(Y, C)}{H(Y) + H(C)}, \quad (21)$$

where Y denotes the ground-truth labels, C denotes the clusters labels, $I(\cdot)$ is the mutual information measure and $H(\cdot)$ the entropy. The second metric used is the *Adjusted Rand Index* (ARI) [35, 36], which is a corrected for chance version of the Rand Index [60] that measures the degree of overlap between two partitions defined as:

$$ARI(Y, C) = \frac{RI(Y, C) - \mathbb{E}[RI(Y, C)]}{\max\{RI(Y, C)\} - \mathbb{E}[RI(Y, C)]}, \quad (22)$$

where $RI(\cdot)$ denotes the Rand Index and $\mathbb{E}[\cdot]$ is the expected value.

5.5 Experimental Setup and Results

We have conducted a comprehensive performance analysis of the proposed DCSS method in comparison to well-studied deep clustering methods such as DCN [31], DEC [43], and IDEC [44]. These methods are designed to facilitate the learning of a cluster-friendly embedded space as also happens with our approach. Furthermore, we have evaluated the performance of k -means [61] both in the original space and in the embedded space (AE+ k -means). The comparison with the latter approach quantifies the performance improvements achieved through the utilization of AE in the clustering procedure. At this point, it should be noted that for a fair comparison between the deep clustering methods, we used the same model architectures for all the methods, since we observed improved clustering results compared to those proposed in the original papers.

In experiments involving k -means, we initialized the algorithm 100 times and retained the clustering solution with the lowest mean sum of squares error. For the remaining methods, which integrate an AE model in the clustering procedure, we conducted each experiment 10 times. In the context of deep clustering methods, an AE pre-training phase (ignoring the clustering loss) took place. For image datasets, we pretrained the AE for 100 epochs with a learning rate of 1×10^{-3} , while for tabular datasets, we extended the pre-training to 1000 epochs with a learning rate of 5×10^{-4} . During the pre-training phase, a small L_2 regularization of 1×10^{-5} was applied. In the training phase, the deep clustering models were trained for 100 epochs with a learning rate of 5×10^{-4} and no regularization penalty.

A fixed batch size of 256 was considered and the Adam optimizer [62] with the default settings of $\beta_1 = 0.9$ and $\beta_2 = 0.999$ was used in both the pretraining and training phases. Additionally, there are several methodologies to tune the non-clustering (eq. 16) with the clustering loss (eq. 15) [19] during training. We choose the most simplistic and typical approach by setting our hyper-parameters to a small values that balances the two losses. Specifically, we used $\lambda_1 = 0.01$ and $\lambda_2 = 0.01$. Finally, to initialize the centers of the RBF layer, we apply k -means in the embeddings of the pretrained AE, while σ was initialized to a small positive value.

In Table 2, we present the average performance in terms of NMI and ARI along with the standard deviation for each method and dataset. As anticipated, the clustering performance of k -means improves when projecting the data to low-dimensional embedded space, as shown in the AE+ k -means compared to k -means results. In general, the performance of DEC is better than that of DCN in all datasets except HAR and WVF-v1. At the same time, we can observe that IDEC slightly outperforms the DEC method in most cases, indicating that some improvement might be obtained by using the decoder part in the clustering optimization procedure. Finally, the results demonstrate the superiority of the proposed DCSS method across all datasets. Concerning the NMI measure, there is a significant improvement ranging from 0.03 to 0.07. In addition, the ARI measure shows an improvement ranging from 0.03 to 0.06. These results indicate that soft silhouette serves as a more suitable deep clustering objective function capable of providing cluster-friendly representations. This is attributed to its optimization approach, which aims for compact and well-separated clusters.

In Figure 3, we present image clustering results using the DCSS method on datasets BL (A-J), BL (K-T), BL (U-Z), and E-MNIST. Images in the same row are assigned to the same cluster and are placed with decreasing cluster assignment probability, progressing from the leftmost (high probability) to the rightmost (low probability) columns. It is obvious that more representative images are assigned higher probability values.



Figure 3: Image clustering results on various datasets. In each sub-figure, rows correspond to different clusters. In each row the images are presented from left to right with decreasing cluster membership probability.

6 Conclusions

In this paper, we have proposed soft silhouette, an extension of the widely used silhouette score that accounts for probabilistic clustering assignments. Next, we have considered soft silhouette as a differentiable clustering objective function and propose the DCSS deep clustering methodology that constitutes an autoencoder-based approach suitable for optimizing the soft silhouette score. The DCSS method guides the learned latent representations to form both compact and well-separated clusters. This property is crucial in real-world applications, as targeting both compactness and separability ensures that the resulting clusters are not only densely packed but also distinct from each other.

The proposed method has been tested and compared with well-known deep clustering methods on various benchmark datasets, yielding very satisfactory results. The experimental study indicates that soft silhouette constitutes as a more suitable deep clustering objective function capable of enhancing the learned representations of the embedded space for clustering purposes.

There are several directions for future work, such as improving the clustering results using data augmentation techniques since it is adopted as an effective strategy for enhancing the learned representations [55, 63]. In addition, more sophisticated models and training methodologies can be used, such as ensemble models [64] or adversarial learning [65]. It is also possible to modify the learning procedure to incorporate self-paced learning [66], since learning the 'easier' data first is expected to improve the clustering results [67–69]. However, our major focus will be on extending the DCCS algorithm for estimating the number of clusters by exploiting unimodality tests as happens in the dip-means [70] and DIPDECK [71] algorithms.

Code Availability

An (early) version of the code and relevant experiments will soon be available in the following github repository: <https://github.com/gvardakas/Soft-Silhouette>.

References

- [1] GM Harshvardhan, Mahendra Kumar Gourisaria, Manjusha Pandey, and Siddharth Swarup Rautaray. A comprehensive survey and analysis of generative models in machine learning. *Computer Science Review*, 38:100285, 2020.
- [2] Daokun Zhang, Jie Yin, Xingquan Zhu, and Chengqi Zhang. Network representation learning: A survey. *IEEE transactions on Big Data*, 6(1):3–28, 2018.
- [3] Olfa Nasraoui and C-E Ben N’Cir. Clustering methods for big data analytics. *Techniques, Toolboxes and Applications*, 1:91–113, 2019.
- [4] Maurizio Filippone, Francesco Camastra, Francesco Masulli, and Stefano Rovetta. A survey of kernel and spectral methods for clustering. *Pattern recognition*, 41(1):176–190, 2008.
- [5] Anil K Jain. Data clustering: 50 years beyond k-means. *Pattern recognition letters*, 31(8):651–666, 2010.
- [6] Absalom E Ezugwu, Abiodun M Ikotun, Olaide O Oyelade, Laith Abualigah, Jeffery O Agushaka, Christopher I Eke, and Andronicus A Akinyelu. A comprehensive survey of clustering algorithms: State-of-the-art machine learning applications, taxonomy, challenges, and future research prospects. *Engineering Applications of Artificial Intelligence*, 110:104743, 2022.
- [7] Daniel Aloise, Amit Deshpande, Pierre Hansen, and Preyas Popat. Np-hardness of euclidean sum-of-squares clustering. *Machine learning*, 75(2):245–248, 2009.
- [8] James MacQueen et al. Some methods for classification and analysis of multivariate observations. In *Proceedings of the fifth Berkeley symposium on mathematical statistics and probability*, volume 1, pages 281–297. Oakland, CA, USA, 1967.
- [9] Christopher M Bishop. Pattern recognition. *Machine learning*, 128(9), 2006.
- [10] Martin Ester, Hans-Peter Kriegel, Jörg Sander, Xiaowei Xu, et al. A density-based algorithm for discovering clusters in large spatial databases with noise. In *kdd*, volume 96, pages 226–231, 1996.
- [11] Alex Rodriguez and Alessandro Laio. Clustering by fast search and find of density peaks. *science*, 344(6191):1492–1496, 2014.
- [12] Svante Wold, Kim Esbensen, and Paul Geladi. Principal component analysis. *Chemometrics and intelligent laboratory systems*, 2(1-3):37–52, 1987.

- [13] Daniel D Lee and H Sebastian Seung. Learning the parts of objects by non-negative matrix factorization. *Nature*, 401(6755):788–791, 1999.
- [14] Andrew Y Ng, Michael I Jordan, and Yair Weiss. On spectral clustering: Analysis and an algorithm. In *Advances in neural information processing systems*, pages 849–856, 2002.
- [15] Nicos G Pavlidis, David P Hofmeyr, and Sotiris K Tasoulis. Minimum density hyperplanes. *Journal of Machine Learning Research*, 2016.
- [16] Yoshua Bengio, Aaron Courville, and Pascal Vincent. Representation learning: A review and new perspectives. *IEEE transactions on pattern analysis and machine intelligence*, 35(8):1798–1828, 2013.
- [17] Alex Krizhevsky, Ilya Sutskever, and Geoffrey E Hinton. Imagenet classification with deep convolutional neural networks. *Advances in neural information processing systems*, 25:1097–1105, 2012.
- [18] Yann LeCun, Yoshua Bengio, and Geoffrey Hinton. Deep learning. *nature*, 521(7553):436–444, 2015.
- [19] Elie Aljalbout, Vladimir Golkov, Yawar Siddiqui, Maximilian Strobel, and Daniel Cremers. Clustering with deep learning: Taxonomy and new methods. *arXiv preprint arXiv:1801.07648*, 2018.
- [20] Erxue Min, Xifeng Guo, Qiang Liu, Gen Zhang, Jianjing Cui, and Jun Long. A survey of clustering with deep learning: From the perspective of network architecture. *IEEE Access*, 6:39501–39514, 2018.
- [21] Gopi Nutakki, Behnoush Abdollahi, Wenlong Sun, and Olfa Nasraoui. *An Introduction to Deep Clustering*, pages 73–89. 01 2019.
- [22] Sheng Zhou, Hongjia Xu, Zhuonan Zheng, Jiawei Chen, Jiajun Bu, Jia Wu, Xin Wang, Wenwu Zhu, Martin Ester, et al. A comprehensive survey on deep clustering: Taxonomy, challenges, and future directions. *arXiv preprint arXiv:2206.07579*, 2022.
- [23] Yazhou Ren, Jingyu Pu, Zhimeng Yang, Jie Xu, Guofeng Li, Xiaorong Pu, Philip S Yu, and Lifang He. Deep clustering: A comprehensive survey. *arXiv preprint arXiv:2210.04142*, 2022.
- [24] Ian Goodfellow, Jean Pouget-Abadie, Mehdi Mirza, Bing Xu, David Warde-Farley, Sherjil Ozair, Aaron Courville, and Yoshua Bengio. Generative adversarial nets. In *Advances in neural information processing systems*, pages 2672–2680, 2014.
- [25] Diederik P Kingma and Max Welling. Auto-encoding variational bayes. *arXiv preprint arXiv:1312.6114*, 2013.
- [26] Jie Zhou, Ganqu Cui, Shengding Hu, Zhengyan Zhang, Cheng Yang, Zhiyuan Liu, Lifeng Wang, Changcheng Li, and Maosong Sun. Graph neural networks: A review of methods and applications. *AI open*, 1:57–81, 2020.
- [27] Sudipto Mukherjee, Himanshu Asnani, Eugene Lin, and Sreeram Kannan. Clustergan: Latent space clustering in generative adversarial networks. In *Proceedings of the AAAI Conference on Artificial Intelligence*, volume 33, pages 4610–4617, 2019.
- [28] Zhuxi Jiang, Yin Zheng, Huachun Tan, Bangsheng Tang, and Hanning Zhou. Variational deep embedding: An unsupervised and generative approach to clustering. *arXiv preprint arXiv:1611.05148*, 2016.
- [29] Jianwei Yang, Devi Parikh, and Dhruv Batra. Joint unsupervised learning of deep representations and image clusters. In *Proceedings of the IEEE conference on computer vision and pattern recognition*, pages 5147–5156, 2016.
- [30] Georgios Vardakas and Aristidis Likas. Neural clustering based on implicit maximum likelihood. *Neural Computing and Applications*, pages 1–14, 2023.
- [31] Bo Yang, Xiao Fu, Nicholas D Sidiropoulos, and Mingyi Hong. Towards k-means-friendly spaces: Simultaneous deep learning and clustering. In *international conference on machine learning*, pages 3861–3870. PMLR, 2017.
- [32] Eréndira Rendón, Itzel Abundez, Alejandra Arizmendi, and Elvia M Quiroz. Internal versus external cluster validation indexes. *International Journal of computers and communications*, 5(1):27–34, 2011.
- [33] Pablo A Estévez, Michel Tesmer, Claudio A Perez, and Jacek M Zurada. Normalized mutual information feature selection. *IEEE Transactions on neural networks*, 20(2):189–201, 2009.
- [34] Nguyen Xuan Vinh, Julien Epps, and James Bailey. Information theoretic measures for clusterings comparison: Variants, properties, normalization and correction for chance. *Journal of Machine Learning Research*, 11(95):2837–2854, 2010.
- [35] Lawrence Hubert and Phipps Arabie. Comparing partitions. *Journal of classification*, 2(1):193–218, 1985.
- [36] José E Chacón and Ana I Rastrojo. Minimum adjusted rand index for two clusterings of a given size. *Advances in Data Analysis and Classification*, pages 1–9, 2022.

- [37] Joseph C Dunn. A fuzzy relative of the isodata process and its use in detecting compact well-separated clusters. 1973.
- [38] Tadeusz Caliński and Jerzy Harabasz. A dendrite method for cluster analysis. *Communications in Statistics-theory and Methods*, 3(1):1–27, 1974.
- [39] David L Davies and Donald W Bouldin. A cluster separation measure. *IEEE transactions on pattern analysis and machine intelligence*, (2):224–227, 1979.
- [40] Peter J Rousseeuw. Silhouettes: a graphical aid to the interpretation and validation of cluster analysis. *Journal of computational and applied mathematics*, 20:53–65, 1987.
- [41] Olatz Arbelaitz, Ibai Gurrutxaga, Javier Muguerza, Jesús M Pérez, and Iñigo Perona. An extensive comparative study of cluster validity indices. *Pattern recognition*, 46(1):243–256, 2013.
- [42] Laurens Van der Maaten and Geoffrey Hinton. Visualizing data using t-sne. *Journal of machine learning research*, 9(11), 2008.
- [43] Junyuan Xie, Ross Girshick, and Ali Farhadi. Unsupervised deep embedding for clustering analysis. In *International conference on machine learning*, pages 478–487. PMLR, 2016.
- [44] Xifeng Guo, Long Gao, Xinwang Liu, and Jianping Yin. Improved deep embedded clustering with local structure preservation. In *Ijcai*, pages 1753–1759, 2017.
- [45] Chunfeng Song, Feng Liu, Yongzhen Huang, Liang Wang, and Tieniu Tan. Auto-encoder based data clustering. In *Progress in Pattern Recognition, Image Analysis, Computer Vision, and Applications: 18th Iberoamerican Congress, CIARP 2013, Havana, Cuba, November 20-23, 2013, Proceedings, Part I 18*, pages 117–124. Springer, 2013.
- [46] Martin Dietrich Buhmann. Radial basis functions. *Acta numerica*, 9:1–38, 2000.
- [47] Lawrence K Saul and Sam T Roweis. Think globally, fit locally: unsupervised learning of low dimensional manifolds. *Journal of machine learning research*, 4(Jun):119–155, 2003.
- [48] Joshua B Tenenbaum, Vin de Silva, and John C Langford. A global geometric framework for nonlinear dimensionality reduction. *science*, 290(5500):2319–2323, 2000.
- [49] Yann LeCun and Corinna Cortes. MNIST handwritten digit database. 2010.
- [50] M Emre Celebi, Hassan A Kingravi, and Patricio A Vela. A comparative study of efficient initialization methods for the k-means clustering algorithm. *Expert systems with applications*, 40(1):200–210, 2013.
- [51] Gregory Cohen, Saeed Afshar, Jonathan Tapson, and Andre Van Schaik. Emnist: Extending mnist to handwritten letters. In *Int’l Joint Conf. on Neural Networks*, pages 2921–2926. IEEE, 2017.
- [52] Erhan Bulbul, Aydin Cetin, and Ibrahim Alper Dogru. Human activity recognition using smartphones. In *2018 2nd International Symposium on Multidisciplinary Studies and Innovative Technologies (ISMSIT)*, pages 1–6, 2018.
- [53] Dheeru Dua and Casey Graff. UCI machine learning repository, 2017.
- [54] Laurens Van Der Maaten. Learning a parametric embedding by preserving local structure. In *Artificial intelligence and statistics*, pages 384–391. PMLR, 2009.
- [55] Xifeng Guo, En Zhu, Xinwang Liu, and Jianping Yin. Deep embedded clustering with data augmentation. In *Asian conference on machine learning*, pages 550–565. PMLR, 2018.
- [56] Yazhou Ren, Ni Wang, Mingxia Li, and Zenglin Xu. Deep density-based image clustering. *Knowledge-Based Systems*, 197:105841, 2020.
- [57] Wengang Guo, Kaiyan Lin, and Wei Ye. Deep embedded k-means clustering. In *2021 International Conference on Data Mining Workshops (ICDMW)*, pages 686–694. IEEE, 2021.
- [58] Vinod Nair and Geoffrey E Hinton. Rectified linear units improve restricted boltzmann machines. In *Proceedings of the 27th international conference on machine learning (ICML-10)*, pages 807–814, 2010.
- [59] Kaiming He, Xiangyu Zhang, Shaoqing Ren, and Jian Sun. Delving deep into rectifiers: Surpassing human-level performance on imagenet classification. In *Proceedings of the IEEE international conference on computer vision*, pages 1026–1034, 2015.
- [60] William M Rand. Objective criteria for the evaluation of clustering methods. *Journal of the American Statistical association*, 66(336):846–850, 1971.
- [61] Stuart Lloyd. Least squares quantization in pcm. *IEEE transactions on information theory*, 28(2):129–137, 1982.

- [62] Diederik P Kingma and Jimmy Ba. Adam: A method for stochastic optimization. *arXiv preprint arXiv:1412.6980*, 2014.
- [63] Xiaozhi Deng, Dong Huang, Ding-Hua Chen, Chang-Dong Wang, and Jian-Huang Lai. Strongly augmented contrastive clustering. *Pattern Recognition*, 139:109470, 2023.
- [64] Séverine Affeldt, Lazhar Labiod, and Mohamed Nadif. Spectral clustering via ensemble deep autoencoder learning (sc-edae). *Pattern Recognition*, 108:107522, 2020.
- [65] Xu Yang, Cheng Deng, Kun Wei, Junchi Yan, and Wei Liu. Adversarial learning for robust deep clustering. *Advances in Neural Information Processing Systems*, 33:9098–9108, 2020.
- [66] M Kumar, Benjamin Packer, and Daphne Koller. Self-paced learning for latent variable models. *Advances in neural information processing systems*, 23, 2010.
- [67] Fengfu Li, Hong Qiao, and Bo Zhang. Discriminatively boosted image clustering with fully convolutional autoencoders. *Pattern Recognition*, 83:161–173, 2018.
- [68] Xifeng Guo, Xinwang Liu, En Zhu, Xinzhong Zhu, Miaomiao Li, Xin Xu, and Jianping Yin. Adaptive self-paced deep clustering with data augmentation. *IEEE Transactions on Knowledge and Data Engineering*, 32(9):1680–1693, 2019.
- [69] Kai Zhang, Chengyun Song, and Lianpeng Qiu. Self-paced deep clustering with learning loss. *Pattern Recognition Letters*, 171:8–14, 2023.
- [70] Argyris Kalogeratos and Aristidis Likas. Dip-means: an incremental clustering method for estimating the number of clusters. *Advances in neural information processing systems*, 25, 2012.
- [71] Collin Leiber, Lena GM Bauer, Benjamin Schelling, Christian Böhm, and Claudia Plant. Dip-based deep embedded clustering with k-estimation. In *Proceedings of the 27th ACM SIGKDD Conference on Knowledge Discovery & Data Mining*, pages 903–913, 2021.